10

MHD Oscillations in the Earth's Magnetotail: Theoretical Studies

A. S. Leonovich, V. A. Mazur, and D. A. Kozlov

10.1. INTRODUCTION

In studies of hydromagnetic oscillations of the Earth's magnetosphere (geomagnetic pulsations), it is often considered as a giant resonator for MHD waves. A wide range of possibilities exist inside the magnetosphere for the generation, propagation, and interaction of these waves. Various magnetospheric processes are often accompanied by the generation of geomagnetic pulsations. In this regard the magnetospheric MHD oscillations have long attracted the attention of researchers, both observers and theorists (see *Southwood and Hughes* [1983]; *Hughes* [1994]; *Kangas et al*. [1998]). Let us note that the theoretical description of MHD oscillations in an inhomogeneous magnetospheric plasma is very important for establishing links between geomagnetic pulsations and magnetospheric processes. This is why so much attention in the studies of magnetospheric ULF oscillations is devoted to their theoretical investigations. The basic theoretical concepts of magnetospheric MHD oscillations can be found in the reviews by *Pilipenko* [1990]; *Allan and Poulter* [1992]; *Stasiewicz et al*. [2000]; *Villante* [2007].

The recent appearance of multi-spacecraft observations has made it possible to examine in much detail MHD oscillations generated and propagating in the Earth's magnetosphere [*Foullon et al*., 2008; *Agapitov and Cheremnykh* 2013]. This in turn requires a thorough theoretical research into such oscillations. Various branches of MHD oscillations interact in an inhomogeneous magnetospheric plasma, which creates a complex picture of wave fields.

The magnetotail ULF oscillations have their own features. The presence of the current and plasma sheets in this region impacts the structure and spectra of Alfvén waves [*Rankin et al*., 2000; *Keiling*, 2009]. During geomagnetic substorms, current disruption processes occur generating an impulse of fast magnetosonic (FMS) waves that are transformed into Alfvén waves at the resonance magnetic shells [*Allan and Wright*, 1998]. The Alfvén waves generated in the process look like pulses of field-aligned currents observable as Pi2 geomagnetic pulsations [*Lee and Lysak*, 1999]. Resonant transformation of FMS waves excited in the plasma sheet into the Alfvén waves can also occur at the plasma sheet boundary [*Lysak et al*., 2009]. Alfvén waves generated in various magnetospheric processes can accelerate the charged particles in the auroral ionosphere and trigger structured auroras [*Stasiewicz et al*., 2000].

Similar to Alfvén waves, slow magnetosonic (SMS) waves propagate more or less along the geomagnetic field lines. These branches can interact on magnetic shells crossing the magnetotail current sheet [*Ohtani et al*., 1989]. Such coupled oscillations can become unstable on curved field lines in the presence of an outward pressure gradient of the background plasma [*Liu*, 1997; *Cheremnykh and Parnowski*, 2006; *Mazur et al*., 2013]. This ("ballooning") instability is assumed to be able to lead to reconnection of magnetic field lines at the initial stage of geomagnetic substorms [*Cheng*, 2004; *Saito et al*., 2008].

The geomagnetic tail can be a waveguide for FMS waves [*Mann et al*., 1999]. Eigenmodes in such waveguide can be excited by a shear plasma flow instability at the magnetopause (Kelvin–Helmholtz instability). An increased wave amplitude due to such an instability when MHD waves pass through a shear flow layer at the magnetopause was studied in *McKenzie* [1970]. The conditions for the Kelvin–Helmholtz instability due to the

Institute of Solar-Terrestrial Physics SB RAS, Irkutsk, Russia

Low-Frequency Waves in Space Plasmas, Geophysical Monograph 216, First Edition.
Edited by Andreas Keiling, Dong-Hun Lee, and Valery Nakariakov.

plasma velocity shear are rarely fulfilled in the mantle-like boundary layer. However, unstable oscillations may arise there due to a resonant flow instability (RFI) [*Hasegawa et al*., 2006]. These oscillations develop in the plasma boundary layer with rather strong variations in Alfvén speed and sound speed [*ErdéLyi and Taroyan*, 2003].

FMS waves penetrating from the solar wind into the magnetosphere excite the resonant Alfvén and SMS waves in the magnetopause boundary layer. Due to the high dissipativity of SMS waves, an efficient transfer occurs of energy and momentum to the background plasma ions. As a result cells with reverse plasma convection can form in magnetospheric regions adjacent to the magnetopause [*Leonovich and Kozlov*, 2013a]. Recently discovered kink-like oscillations in the magnetotail current sheet [*Zhang et al*., 2002] suggest that these oscillations are unlike any known MHD oscillations, and thus they demand special examination.

10.2. MHD WAVES ASSOCIATED WITH A SHEAR FLOW AT THE MAGNETOPAUSE

A shear flow instability on the magnetopause (the Kelvin–Helmholtz instability) has long been regarded as a possible source of MHD oscillations in the Earth's magnetosphere [*McKenzie*, 1970; *Mishin*, 1981; *Miura and Pritchett*, 1982]. Until recently, however, there had been no direct observations of magnetospheric oscillations that could be directly identified as such unstable MHD modes. It was only very recently that the THEMIS and Double Star spacecraft recorded oscillations that can be seen as FMS surface waves driven by a Kelvin–Helmholtz instability [*Volwerk et al*., 2007]. The amplitude of these oscillations decreases outward of the magnetopause and increases in the direction of their tailward propagation.

Similar THEMIS spacecraft observations are presented in *Agapitov et al*. [2009], where the propagation velocity of unstable oscillations (~ 200 km/s) coincides with the expected propagation velocity of FMS surface waves. Besides, the THEMIS 5 spacecraft inside the magnetosphere registered a narrowly localized jump in the oscillation amplitude identifiable as an Alfvén wave excited by the field line resonance (FLR) mechanism [*Agapitov et al*., 2009]. This can be regarded as the first direct evidence for the existence of the classical FLR [*Tamao*, 1965; *Chen and Hasegawa*, 1974, *Radoski*, 1974; *Southwood*, 1974; *Leonovich*, 2001].

Spacecraft observations combined with local ground magnetometer network data have allowed wave energy flow to be estimated from the magnetopause to the ionosphere through the FLR mechanism [*Hartinger et al*., 2011]. The data suggest that energy absorption in the ionosphere is a significant damping mechanism for magnetospheric MHD waves.

Most theoretical studies of shear flow instabilities employ models based on a tangential discontinuity of the medium parameters. In such models, the parameters change abruptly during a transition from the homogeneous half-space with motionless plasma to the other half-space with moving plasma. The plasma in the magnetosphere is, however, strongly inhomogeneous. This fact has given an impetus to models of the medium where the plasma parameters in the half-space simulating the magnetosphere change in the direction transverse to the shear layer direction. The easiest way to model such inhomogeneity is to place a reflecting wall at some distance from the shear layer [*Miura*, 1992; *Leonvich and Mishin*, 2005; *Turkakin et al*., 2014].

These models allow for the presence of a waveguide for FMS waves propagating between the reflecting wall and the magnetopause [*Mann et al*., 1999]. Since the magnetopause is only a partially reflective wall (a free boundary), the basic harmonic in such a waveguide is a quarter-wave, meaning its frequency is lower than in the waveguide with two perfectly reflecting walls. That frequency (~ 1 mHz) falls into the range of "magic frequencies." However, a threshold for the plasma velocity shift at the magnetopause exists for FMS waves, which when exceeded gives rise to their instability. Under certain conditions, however, this threshold disappears [*Turkakin et al*., 2013].

More complicated are models that include a monotonic change of the medium parameters in the half-space describing the magnetosphere [*Walker*, 2005]. In such models the role of a reflecting wall is played by the surface separating the transparency from the opacity regions for FMS waves in the magnetosphere. In the opacity region behind the turning point, there is a resonance surface for Alfvén waves partially absorbing the energy of the FMS wave propagating in the magnetospheric waveguide [*Mazur and Chuiko*, 2011].

Such a waveguide can be excited by an FMS wave incident on the magnetopause from the magnetosheath. The reflection coefficient in this case has pronounced peaks at frequencies corresponding to the magnetospheric waveguide eigenmode frequencies [*Mazur*, 2010]. The maximum reflection coefficient can exceed unity, that means the wave reflected from the shear layer has an amplitude greater than the incident wave. Increased amplitude is due to the energy transferred from the plasma shear flow to the wave. Such a wave is referred as a negative energy wave [*Mann et al*., 1999; *Walker*, 2005; *Mazur and Chuiko*, 2013].

Yet another group of models are those with a smooth transition layer between the magnetosheath with moving plasma and a magnetosphere [*Miura*, 1992; *Leonovich*, 2011a]. In these models the resonance surfaces for Alfvén and SMS waves appear not only in the opacity regions of FMS waves in the magnetosphere but also in

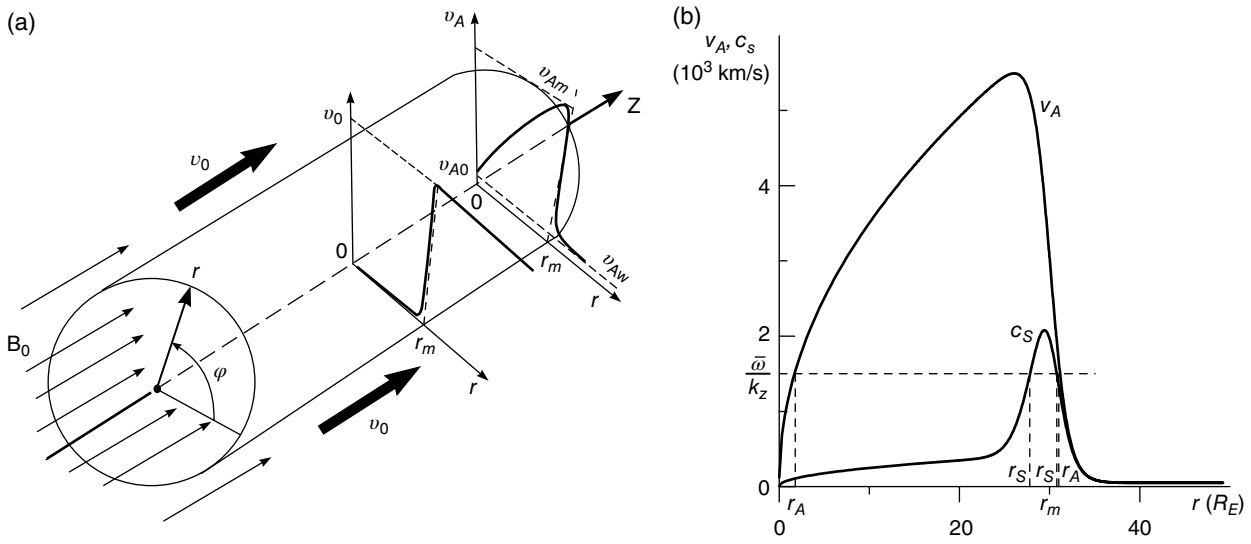

Figure 10.1 (a) Model of the geomagnetic tail in the form of a plasma cylinder wrapped around by the solar wind flow. (b) Radial distribution of the Alfvén, v_A, and SMS wave speed, c_s, as determined from the condition that the plasma configuration is in equilibrium. The Alfvén resonance point (r_A) and the magnetosonic resonance point (r_s) correspond to $\bar{\omega}/k_z = v_A(r_A)$ and $\bar{\omega}/k_z = c_s(r_s)$.

the magnetopause transition layer. FMS wave energy is absorbed at each of those surfaces, which affects their growth rate and spatial amplitude distribution.

The problem of Kelvin–Helmholtz instability developing at the magnetopause wrapped around by the solar wind flow was solved in *Leonovich* [2011a, b] by way of a cylindrical model of the magnetotail with an inhomogeneous plasma distribution over the radius and a boundary in the form of a smooth transition layer (see Figure 10.1). The magnetopause radius in this model is $r = r_m = 30R_E$. This model includes all of the above-mentioned features of Kelvin–Helmholtz instability in an inhomogeneous magnetosphere. The plasma distribution typical of the magnetotail lobes is such that the plasma cylinder can act as a waveguide for the FMS waves, and turning points for the FMS waves appear in the plasma cylinder for any plasma distribution over the radius.

Such a model ignores the presence of the current sheet separating the magnetotail lobes. The current sheet plays a key role in the propagation of small-scale (compared to the sheet thickness) MHD oscillations [*Allan and Wright*, 1998; *Lysak et al*., 2009]. For large-scale oscillations, it can be regarded as thin so that its presence can be neglected in the first approximation.

Let us consider the harmonic of a wave in the form $\exp(ik_z z + im\phi - i\omega t)$, where k_z is the component of the wave vector in the z axis direction, $m = 0,1,2,\ldots$ is the azimuthal wave number, ω is the wave frequency. The equation describing the radial displacement, ζ, of a plasma element has the form [*Leonovich*, 2011b]:

$$\frac{\partial}{\partial r}\left(\frac{\rho_0\Omega^2}{k_r^2}\frac{1}{r}\frac{\partial r\zeta}{\partial r}\right) + \rho_0\Omega^2\zeta = 0 \qquad (10.1)$$

where $v_r = \mathrm{d}\zeta/\mathrm{d}t \equiv \partial\zeta/\partial t + (\mathbf{v_0}\nabla)\zeta$ is the radial velocity component, $\mathbf{v}_0$ is the plasma velocity, ρ_0 is the plasma density, $\Omega^2 = \bar{\omega}^2 - k_z^2 v_A^2$, $v_A = B_0/\sqrt{4\pi\rho_0}$ is the Alfvén speed, B_0 is magnetic field strength, $\bar{\omega} = \omega - k_z v_0$,

$$k_r^2 = \frac{\bar{\omega}^4}{\bar{\omega}^2\left(v_A^2 + v_s^2\right) - k_z^2 v_A^2 v_s^2} - k_z^2 - \frac{m^2}{r^2}$$

is the square of the wave vector radial component in the WKB approximation, $v_s = \sqrt{\gamma P_0/\rho_0}$ is the sound speed in plasma, P_0 is plasma pressure, γ is adiabatic index.

Equation (10.1) has singularities at the resonance surfaces, where the coefficient of the highest derivative vanishes. This occurs at points where $\bar{\omega}^2 = k_z^2 v_A^2$ (the Alfvén resonance point) and $\bar{\omega}^2 = k_z^2 c_s^2$ (the magnetosonic resonance point, $c_s = v_A v_s/\sqrt{v_A^2 + v_s^2}$ is the SMS wave speed). MHD wave energy is transferred to the background plasma near the resonance surfaces. Note that since, in an inhomogeneous plasma, all MHD modes are interrelated, (10.1) describes the unified MHD oscillation field. Away from the resonance surfaces, the oscillation field can be regarded as an FMS wave; near the Alfvén resonance surface its polarization is similar to the Alfvén wave polarization in a homogeneous plasma, while near

the magnetosonic resonance surface it is similar to the SMS wave polarization.

In the instability problem for the MHD waves in question, the boundary conditions are reduced to the requirements that their amplitude be finite on the plasma cylinder axis ($r = 0$) and only waves carrying the energy away from the magnetopause shear layer be found at infinity ($r \to \infty$). The last boundary condition can be formulated as

$$\frac{\partial \zeta}{\partial r} = ik_r \zeta \tag{10.2}$$

where the sign of $k_r = \pm\sqrt{k_r^2(r \to \infty)}$ is defined by the condition $\mathrm{Re}(v_{gr}) > 0$, with $v_{gr} = (\partial k_r / \partial \omega)^{-1}$ as the group velocity of FMS waves. Figure 10.2a gives an example of a calculated oscillation field having two resonance surfaces in the magnetopause transition layer: for Alfven ($r = r_A$) and SMS waves ($r = r_S$). In the figure, the singularities of the wave field (logarithmic singularities for the ζ function) on resonance surfaces are clearly evident in the magnetopause transition layer, as in FLR theory. We found that the waveguide modes propagating in the magnetotail lobes can become unstable in the model only for a large enough plasma velocity shift at the magnetopause $v_0 > v_{Am}$, where $v_{Am} \approx 6000$ km/s is the Alfvén speed in the magnetospheric regions adjacent to the magnetopause. Such high-speed solar wind flows are nonexistent at the Earth's orbit. This conclusion is fully consistent with the one in *Fujita et al.* [1996], employing Cartesian coordinates for a 1D inhomogeneous magnetosphere model.

The surface waves driven by the Kelvin–Helmholtz instability have a lower threshold for the plasma velocity shift. However, there is one exception. The threshold disappears for oscillations with $\mathbf{k}_t \perp \mathbf{B_0}$, where $\mathbf{k}_t$ is the wave vector component along the shear layer [*Leonvich and Mishin*, 2005]. In this case, the Kelvin–Helmholtz instability develops in a way similar to the classical fluid shear flow. Such conditions are achieved, for example, in the region of the low-latitude boundary layer (LLBL) for the axisymmetric mode ($m = 0$) [*Hasegawa et al.*, 2006; *Foullon et al.*, 2008].

In the model describing the magnetotail lobes, the same conditions are reached for oscillations with $k_z \to 0$. The unstable oscillations propagate in the azimuthal direction across the magnetic field lines. For these oscillations, on the contrary, an upper threshold appears in shear velocity, exceeding which the surface modes become stable. If we consider the shear layer as a tangential discontinuity, the range of shear velocities for which the surface wave instability develops is

$$0 < v_0 < v_{Aw}\sqrt{1 - \frac{B_{0w}^2 m}{B_{0m}^2\left(m^2+1\right)}}$$

where $m = 1, 2, 3, \ldots$ is the azimuthal wave number, B_{0m} is the magnetic field in the magnetospheric region adjacent to the magnetopause, B_{0w} is the magnetic field in the magnetosheath. In other words, an unstable surface wave cannot be generated when the solar wind velocity exceeds the maximum Alfvén speed in the magnetopause transition layer. As for the azimuthal harmonic $m = 0$, this harmonic is unstable almost throughout the entire range of the shear velocities, even though its growth rate is much smaller than

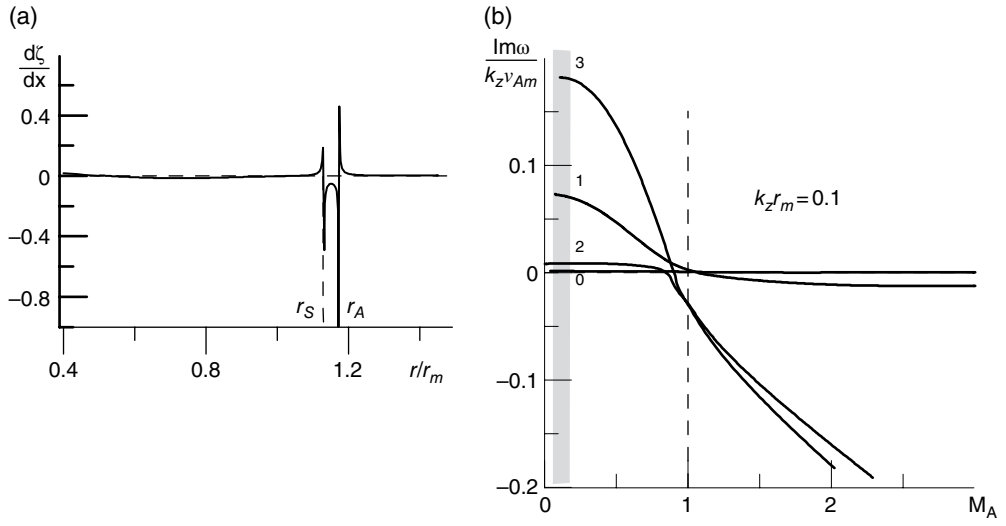

Figure 10.2 (a) Radial distribution of the oscillation field with two resonance surfaces, for the Alfvén waves ($r = r_A$) and SMS waves ($r = r_s$). (b) Alfvénic Mach number ($M_A = \upsilon_0 / \upsilon_{Am}$) dependence of the surface mode growth rate for azimuthal harmonics with m =0, 1, 2, 3. The vertical gray bar corresponds to the velocity range of the solar wind in the Earth's orbit.

that for the other harmonics. We performed a numerical integration of (10.1) with boundary conditions (10.2) for a magnetospheric model with a smooth transition layer at the magnetopause. Figure 10.2b shows the dependence of the growth rate for different azimuthal harmonics on the Alfvénic Mach number $M_A = v_0/v_{Am}$ for the finite value of $k_z r_m = 0.1$, which corresponds to oscillation frequency $f \approx 0.1$ mHz. The vertical gray bar shows the solar wind velocity range in the Earth's orbit. Interestingly, the amplitude of such surface oscillations remains virtually unchanged, with the radius inside the magnetosphere. Therefore this instability can be regarded as a possible excitation mechanism for global modes in the magnetotail.

The same cylindrical model magnetosphere was used in *Leonovich* [2012] to successfully solve the problem of the momentum transfer from the solar wind to the magnetospheric plasma ions via FMS waves. Unfortunately, this model does not take into account the presence of a current sheet separating the tail into two lobes. Using it for the above wave processes can be justified as follows. The magnetotail current sheet can be considered as thin, for global oscillations, with virtually no effect on their structure. For oscillations penetrating from the solar wind into the magnetosphere, all processes we are interested in occur in regions adjacent to the magnetopause. The current sheet is located far enough from these regions so that its presence can be neglected.

The momentum is transferred at resonance surfaces for SMS waves excited by FMS waves penetrating into the magnetosphere from the solar wind. We examined how the ion distribution function varied under the impact of SMS waves with a stochastic phase distribution. The following diffusion equation was used to describe this process (see *Akhiezer et al*. [1975]):

$$\frac{\partial f}{\partial t} \approx \frac{\partial}{\partial v_\parallel} D \frac{\partial f}{\partial v_\parallel} \tag{10.3}$$

It is applicable for waves with linear dispersion similar to SMS waves $\omega \approx k_\parallel c_s$. Here $f(v_\parallel, v_\perp, t)$ is the ion velocity distribution function, $v_{\parallel,\perp}$ are the ion velocities along and across magnetic field lines,

$$D \approx \frac{\pi}{4} \frac{v_\perp^4}{v_\parallel B_0^2} \sum_{m=0}^{\infty} \int_0^\infty \left\langle \left| \nabla_r B_r(r, m, k_z = \omega / v_\parallel, \omega) \right| \right\rangle^2 d\omega \tag{10.4}$$

is the diffusion coefficient related to the effect of waves in resonance with the background plasma ions ($\omega = k_z v_\parallel$, i.e., $v_\parallel = c_s$), $B_r = ik_z B_0 \zeta$ is the magnetic field r-component of resonant SMS oscillations.

The equilibrium Maxwellian distribution function

$$f\left(v_\parallel, v_\perp\right) = \frac{n_0}{\pi^{3/2} v_{Ti}^3} \exp\left(-\frac{v_\parallel^2 + v_\perp^2}{v_{Ti}^2} \right)$$

is used as the initial condition for solving (10.3), where n_0 is the plasma ion concentration, $v_{Ti} = \sqrt{2T_i / m_i}$ is ion thermal velocity. Equation (10.3) can be integrated with respect to $v_\perp$, resulting in

$$\frac{\partial \bar{f}}{\partial t} \approx \frac{\partial}{\partial v_\parallel} \bar{D} \frac{\partial \bar{f}}{\partial v_\parallel} \tag{10.5}$$

where

$$\bar{f}\left(v_\parallel\right) = \int_0^{2\pi} d\phi \int_0^\infty v_\perp f\left(v_\parallel, v_\perp\right) dv_\perp$$

$$\bar{D} = \frac{1}{\pi v_{Ti}^2} \int_0^{2\pi} d\phi \int_0^\infty v_\perp D e^{-v_\perp^2 / v_{Ti}^2} dv_\perp$$

Multiplying (10.5) on the left by $\bar{f}$ and integrating over $v_\parallel$, we obtain

$$\frac{1}{2} \frac{\partial}{\partial t} \int_{-\infty}^{\infty} \bar{f}^2 dv_\parallel \approx -\int_{-\infty}^{\infty} \bar{D} \left(\frac{\partial \bar{f}}{\partial v_\parallel} \right)^2 dv_\parallel \tag{10.6}$$

This implies that if a new equilibrium state is reached in the plasma ($\partial \bar{f} / \partial t = 0$) at the t asymptotic, then a plateau must form on the distribution function ($\partial \bar{f} / \partial v_\parallel = 0$) for those $v_\parallel$ ranges where $\bar{D}$ is nonzero.

Analysis of possible $k_\parallel$ ranges within which the solar wind is a transparency region for FMS waves, and SMS resonance surfaces exist in the magnetosphere, arrives at the following conclusion. There are three ranges where a plateau forms on the distribution function $\bar{f}$: $-c_{s\max} < v_\parallel < -c_{s\min}$, $c_{s\min} < v_\parallel < v_2$, and $v_1 > v_\parallel > c_{s\max}$, where $c_{s\min} \approx 8$ km/s is achieved on the plasma cylinder axis and $c_{s\max} \approx 2000$ km/s near the transition layer, $v_1 = v_0 + v_{sw}, v_2 = v_0 - v_{sw}$, where $v_{sw} \approx 177$ km/s is the sound speed in the magnetosheath.

The $c_{s\min} < v_\parallel < v_2$ area corresponds to "downstream" FMS waves, while the two other areas correspond to "upstream" FMS waves in the solar wind. The corresponding $\bar{f}(v_\parallel)$ distribution is presented in Figure 10.3a. Since the distribution function becomes asymmetric over $v_\parallel$, the previously motionless magnetospheric plasma achieves an average velocity.

$$\bar{v}_0 = \frac{1}{n_0} \int_{-\infty}^{\infty} v_\parallel \bar{f}(v_\parallel) dv_\parallel$$

Variations in the radial distribution of the plasma velocity under the impact of MHD waves are shown in Figure 10.3b. In the regions adjacent to the magnetopause, a plasma flow is seen to appear directed against the solar wind velocity. In the high-latitude magnetosphere, this effect manifests itself as reverse plasma convection cells during periods of prolonged Northern B_z component of the IMF, when the

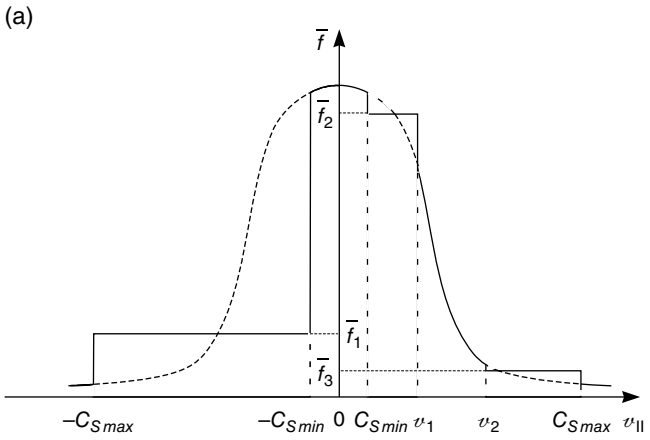

Figure 10.3 (a) "Plateau" formation on the plasma ion distribution function $\bar{f}$ under the impact of MHD waves penetrating into the magnetotail lobes from the magnetosheath. (b) Plasma flow velocity $v_0 + \bar{v}_0$ distribution over radius, in the magnetosheath ($r > r_m$) and in the magnetosphere ($r < r_m$), where v_0 is the velocity of undisturbed solar wind flow, $\bar{v}_0$ is the change in the plasma velocity due to a FMS wave flux into the magnetosphere. Curves 1, 2, 3 correspond to $v_0 = 200, 400, 800$ km/s.

mechanism of magnetospheric convection associated with magnetic reconnection at the magnetopause is missing [*Sergeev et al*., 1996; *Förster et al*., 2008].

10.3. OSCILLATIONS WITH A DISCRETE SPECTRUM OF "MAGIC FREQUENCIES"

A most interesting phenomenon investigated for the past two decades are ULF oscillations with a discrete spectrum. These oscillations were first registered on ground-based networks of HF radars and magnetometers [*Ruohoniemi et al*., 1991; *Samson et al*., 1992]. Due to the repeatability of the frequency spectrum (0.8, 1.3, 1.9, 2.6, … mHz) in various observations and its stability in each of these observations, they were called "magic" frequencies. Such oscillations are recorded usually in the midnight–morning sector of the magnetosphere at 60° to 80° latitudes. Oscillations with similar spectral characteristics were recently discovered by spacecraft near the dayside magnetopause [*Plaschke et al*., 2009; *Archer et al*., 2013], and even in the solar wind [*Viall et al*., 2009].

Several theoretical concepts have so far been proposed in order to explain the nature of these oscillations. As assumed in *Samson et al*. [1992], the observed oscillations with a discrete frequency spectrum are the eigenmodes of a waveguide in the magnetotail lobes. Some difficulties are, however, encountered within the confines of such a concept. The main is the fact that the polarization of the observed oscillations is typical of a standing wave rather than of waves traveling through a waveguide [*Samson and Rankin*, 1994].

A mechanism was suggested [*Kepko et al*., 2002; *Viall et al*., 2009] for the "magic frequency" spectrum oscillations penetrating from the solar wind directly to the magnetosphere. These oscillations are considered [*Plaschke et al*., 2009; *Archer et al*., 2013] as the eigenmodes of Alfvén waves excited at the magnetopause by pulses due to solar wind inhomogeneities. Note the difficulties involved in these two concepts. Since the dayside magnetosphere is an opacity region for the oscillations in question, the oscillation amplitude decreases exponentially from the magnetopause into the magnetosphere [*Leonovich and Mazur*, 2000]. Therefore it is difficult to explain the presence of such oscillations in the midnight–morning sector of the inner magnetosphere, where they were originally discovered.

A magnetospheric resonator model proposed in *Leonovich and Mazur* [2005], *Mazur and Leonovich* [2006] may explain most features of the observed oscillations of the "magic" frequency spectrum. This resonator for FMS waves forms in the near-Earth part of the plasma sheet, where a global minimum in the Alfvén speed distribution exists in the magnetosphere (see Figure 10.4a). The structure and spectrum of these oscillations were determined by solving the following approximate equation:

$$\Delta\Phi + \frac{\omega^2}{v_A^2}\Phi = 0 \tag{10.7}$$

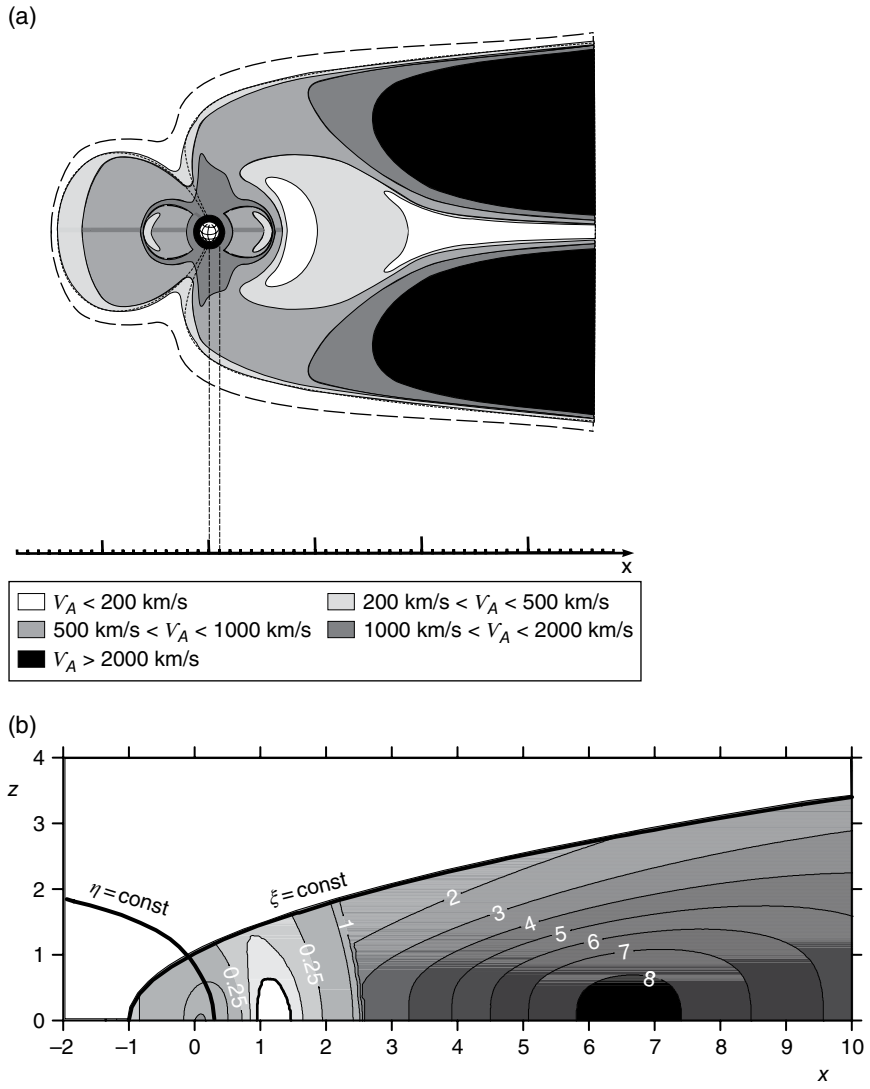

Figure 10.4 (a) Alfvén speed, $v_{A'}$ distribution in the Earth's magnetosphere in the meridional noon–midnight plane. (b) Parabolic coordinates (ξ, η) and Alfvén speed distribution in the parabolic magnetosphere model (in 10^3km/s).

where Φ is any component of the oscillation wave field. The equation successfully describes FMS oscillations in "cold plasma" models, in the WKB approximation, and is also qualitatively applicable to describing FMS oscillations in more complex magnetospheric models.

To describe the resonator in the near-Earth part of the plasma sheet, an axisymmetric parabolic magnetosphere model was used (see Figure 10.4b). The magnetospheric model used in these calculations takes into account the 2D plasma inhomogeneity in the meridional plane. However, it does not describe the real configuration of the plasma sheet in the middle and far magnetotail. Its use for the FMS resonator oscillations relies on the fact that the resonator eigenmodes are localized in the near-Earth part of the plasma sheet, and its middle and far parts are opacity regions for them. Therefore the plasma distribution in these remote regions has little effect on the oscillation structure in the resonator.

The FMS oscillation harmonics have the form $\Phi(\xi, \eta, \phi) = \bar{\Phi}(\xi, \eta)\exp(im\phi)$, where ϕ is the azimuthal angle, $m = 0, 1, 2, \ldots$ is the azimuthal wave number, and ξ, η are the parabolic coordinates in the $\phi = const$ plane. Equation (10.7) in such parabolic coordinates has the form

$$\frac{\partial}{\partial\xi}\xi\frac{\partial\bar{\Phi}}{\partial\xi}+\frac{\partial}{\partial\eta}\eta\frac{\partial\bar{\Phi}}{\partial\eta} + \left[(\xi+\eta)\frac{\omega^2\bar{\sigma}^2}{v_A^2(\xi,\eta)}-\frac{m^2}{4}\left(\frac{1}{\xi}+\frac{1}{\eta}\right)\right]\bar{\Phi}=0 \tag{10.8}$$

where $\bar{\sigma}$ is the distance from the focus (Earth's center) to the vertex of the paraboloid, $\xi = 1$, corresponding to the magnetopause. If the Alfvén speed is presented as

$$v_A^2(\xi, \eta) = \frac{v_{A0}^2}{\bar{\sigma}} \frac{\xi + \eta}{a(\xi) + b(\eta)}$$

where v_{A0} is a constant with the dimension of velocity, and $a(\xi)$ and $b(\eta)$ are any functions of the variables ξ and η, then (10.8) can be shown to be an equation with separable variables. v_{A0}, $a(\xi)$ and $b(\eta)$ can be chosen such as to model the $v_A(\xi,\eta)$ distribution typical of the near-Earth part of the magnetotail, as shown in Figure 10.4b [*Mazur and Leonovich*, 2006].

In solving the problem of eigen-oscillations in a resonator in the near-Earth part of the plasma sheet, we chose the boundary conditions to be in the form of perfectly reflecting oscillations at the magnetopause and the finiteness of their amplitude in the entire domain of existence. Numerical integration of (10.8) produced a spectrum of eigenfrequencies $f_{mnl} = \omega_{mnl}/2\pi$, where $l, m, n = 0, 1, 2, 3, \ldots$ are the harmonic wave numbers for each of the parabolic coordinates (ξ, ϕ, η).

An interesting feature of this spectrum is that the eigenfrequencies are not distributed uniformly, but are grouped into clusters. For example, clusters $f_{000} = 0.73$ mHz and $f_{100} = 1.04$ mHz consist of one frequency only. Clusters ($f_{001} = 1.41$, $f_{010} = 1.36$, $f_{200} = 1.32$ mHz) and ($f_{101} = 1.66$, $f_{110} = 1.66$, $f_{300} = 1.59$ mHz) consist of three harmonics with mean frequencies $\bar{f} \approx 1.35$ mHz and $\bar{f} \approx 1.6$ mHz, respectively. The other harmonics can be pooled into clusters with mean frequencies $\bar{f} \approx 1.95$ mHz, $\bar{f} \approx 2.2$ mHz, $\bar{f} \approx 2.6$ mHz, $\bar{f} \approx 3.1$ mHz, and so on.

Clearly, the frequency spectrum found for the resonator under study is quite similar to the spectrum of the observed "magic frequencies." The localization of ground-observed oscillations at latitudes 60° to 80° are easy to explain as well. It is into this ionospheric region that the resonator in the near-Earth part of the plasma sheet is mapped along magnetic field lines. Due to magnetospheric convection, it is shifted to the midnight–morning sector of the magnetosphere.

The following reasonable assumption can be made about the stability of the observed frequencies. Since these oscillations are usually observed under quiet enough geomagnetic conditions ($K_p < 3$), the parameters of the near-Earth part of the plasma sheet remain about the same. A resonator for FMS waves that forms under these conditions always has nearly identical characteristics.

These oscillations are transmitted to the Earth by Alfvén waves excited in the FLR [*Rankin et al.*, 2006; *Kozlov et al.*, 2006]. The typical eigenfrequencies of the toroidal Alfvén waves on the magnetic shells under study ($10 < L < 20$) fall into the basic mode range of the FMS wave resonator [*Sarris et al.*, 2009]. The characteristic wavelengths of the basic harmonics of this resonator are comparable with the transverse magnetospheric scales. Therefore, under certain conditions, oscillations in these harmonics can be observed even at low enough geomagnetic latitudes ($L \sim 4-6$) in the midnight–morning sector of the magnetosphere. These conditions are (1) sufficiently long existence of the resonator (~5–7 hours) as defined by a time interval with small $K_p \sim 1$ and (2) the simultaneous presence of a pumping mechanism in the resonator such as the solar wind flow causing the magnetopause Kelvin–Helmholtz instability.

The following mechanism is suggested to explain the oscillations with spectral peaks at "magic frequencies" in the solar wind and in the dayside magnetosphere. In the localization region of the resonator, its side walls are located near the plasmapause. For this reason the resonator cannot be regarded as ideal. It is partially permeable for the incident oscillations from the solar wind. Its own eigen-oscillation energy also partially escapes to the solar wind [*Leonovich and Mazur*, 2008].

The spectrum of the solar wind oscillations has frequencies corresponding to the resonator eigenfrequencies [*Kepko et al.*, 2002; *Potapov et al.*, 2013]. The resonator may be powered by FMS waves falling from the solar wind onto the magnetopause and may store energy in its eigen-oscillations. Besides, as follows from the results in the previous section, the resonator eigen-modes may be related to the instability of the magnetotail global modes. These oscillations may propagate as surface waves along the plasmapause to the dayside magnetosphere. Since the typical spatial scale of such oscillations is comparable to the magnetospheric scale, the oscillations are observed deep enough in the dayside magnetosphere.

10.4. COUPLED ALFVÉN AND SLOW MAGNETOSONIC WAVES IN THE MAGNETOTAIL

Another type of MHD oscillations typical of the magnetotail is the coupled Alfvén and SMS waves on stretched magnetic field lines passing through the current sheet. Each of these modes can propagate along paths that almost coincide with the magnetic field lines. Under certain conditions this results in their interaction leading to the formation of a coupled mode of MHD oscillations [*Southwood and Saunders*, 1985; *Walker*, 1987; *Voronkov et al.*, 1997].

Particular interest in such coupled modes is also due to the fact that they can become unstable under certain conditions [*Ohtani et al.*, 1989; *Hameiri et al.*, 1991; *Klimushkin et al.*, 2012; *Kozlov et al.*, 2014]. This occurs in the presence of a plasma pressure gradient directed against the curvature radius of the magnetic field lines.

This instability is of a threshold nature and is called a "ballooning instability." It develops when the curvature of magnetic field lines is high enough, which can be achieved in the magnetotail current sheet under pre-substorm conditions. Therefore this instability is regarded as one of the mechanisms leading to magnetic field line reconnection in the near-Earth part of the current sheet at substorm onset [*Liu*, 1997; *Cheng and Lui*, 1998; *Cheng*, 2004; *Zhu and Raeder*, 2014].

Until recently these coupled modes were chiefly the subject of theoretical studies because they are difficult to separate from other MHD oscillation modes during observations. The data of multi-spacecraft systems like THEMIS, Cluster, and Double Star provided the opportunity to analyze oscillations at various closely spaced points, and therefore made it possible to separate different modes of MHD oscillations and study their interrelationships.

Low-frequency MHD oscillations observed at the equator by the GEOTAIL spacecraft after substorm onset were analyzed in detail in *Saito et al*. [2008]. It was shown that the FMS mode is distinguishable enough in observations, but Alfvén and SMS waves are difficult to separate. Both onboard and ground magnetometer observations of pre-substorm Pi2 pulsations are presented in *Keiling* [2012]. Pi2 are regarded in that work as a signature of a pre-substorm ballooning instability at pseudo-breakup stage. An SMS wave with a period of ~30 s was observed by the Cluster satellites in *Cao et al*. (2013), associated with periodic reconnection in the magnetotail. These observations can be considered as the first evidence that unstable coupled MHD modes do exist.

A number of other observations appear to have observed oscillations of this type. Monochromatic (~10 mHz) giant Pg pulsations were observed in *Takahashi et al*. [2011] with polarization typical of standing poloidal Alfvén waves. Simultaneous Alfvén and SMS oscillations in the same frequency range (period ~100 s) were discovered by the THEMIS satellites near the current sheet (distance from the Earth ~$11R_E$) in *Du et al*. [2011]. No significant plasma pressure gradient was observed, making it unlikely for these oscillations to be unstable. Wave-like structures were observed in *Saka et al*. [2014], by an all-sky imager at Dawson City (65.7°ILAT) pre-substorm onset with azimuthal wave number $m \approx 76$ and period $T \sim 120$ s as are typical of coupled MHD modes.

Coupled Alfvén and SMS oscillations in the observations can be identified by specific features in their spatial structure. The total spatial structure of such oscillations was studied in *Leonovich and Kozlov* [2013b, 2014] on magnetic shells with closed magnetic field lines. Those studies addressed the structure of monochromatic waves driven by external ionospheric currents.

Due to the high conductivity of the ionosphere, these oscillations are standing waves along geomagnetic field lines [*Mager et al*., 2009]. They can propagate across magnetic shells in the transparency region located between the poloidal and toroidal resonance surfaces for Alfvén waves. Outside that area are opacity regions where the oscillation amplitude decreases. The coupled modes are waves propagating in the transparency region from the poloidal resonance surface toward the toroidal resonance surface. They are absorbed completely near the toroidal surface due to the finite conductivity of the ionosphere.

The presence of the toroidal resonance surface makes it impossible for poloidal eigen-oscillations (and coupled modes can be classified as such) to exist in magnetospheric regions with monotonically changing medium parameters. The poloidal resonance surface separates the transparency and opacity regions for Alfvén waves in the direction across magnetic shells. As was shown in *Leonovich and Mazur* [1990], both the incident and reflected waves are necessary for constructing the eigenmode structure in the transparency region. However, waves escaping from the poloidal resonance surface are completely absorbed near the toroidal surface so that the incident wave (traveling toward the poloidal surface) is absent [*Leonovich and Mazur*, 1993]. The only chance for poloidal eigenmodes to exist is the presence of a resonator in magnetospheric regions with nonmonotonically changing medium parameters [*Leonovich and Mazur*, 1995].

Here, we will consider oscillations in a magnetotail model with monotonically varying parameters. Figure 10.5 shows the magnetotail axisymmetric model with a ring current sheet used in *Leonovich and Kozlov* [2013b, 2014]. The magnetic field in this model consists of a magnetic dipole in the near-Earth part of the magnetosphere, and the field of an axisymmetric current sheet in its remote regions. This model allows us to calculate the field of the coupled modes in the meridional plane and their instability-related growth rates. This axisymmetric model, of course, only vaguely resembles the real magnetotail, but for azimuthally small-scale oscillations with $m \gg 1$ the large-scale magnetotail structure has little effect on the oscillation structure in the meridional planes. To calculate the field of individual oscillation harmonics, we can therefore use any model with such basic elements as a dipole magnetic field near the Earth, the current sheet stretching the magnetic field lines in the meridional plane, and a balanced large-scale plasma distribution. For the same reason we can ignore the presence of the magnetopause located far from the current sheet.

The oscillation field in this model can be represented as a series of azimuthal harmonics of the form $\exp(ik_2x^2)$, where x^2 is the cyclic coordinate over which the parameters of the medium are homogeneous, k_2 is the azimuthal component of the wave vector (if $x^2 \equiv \varphi$, where ϕ is the

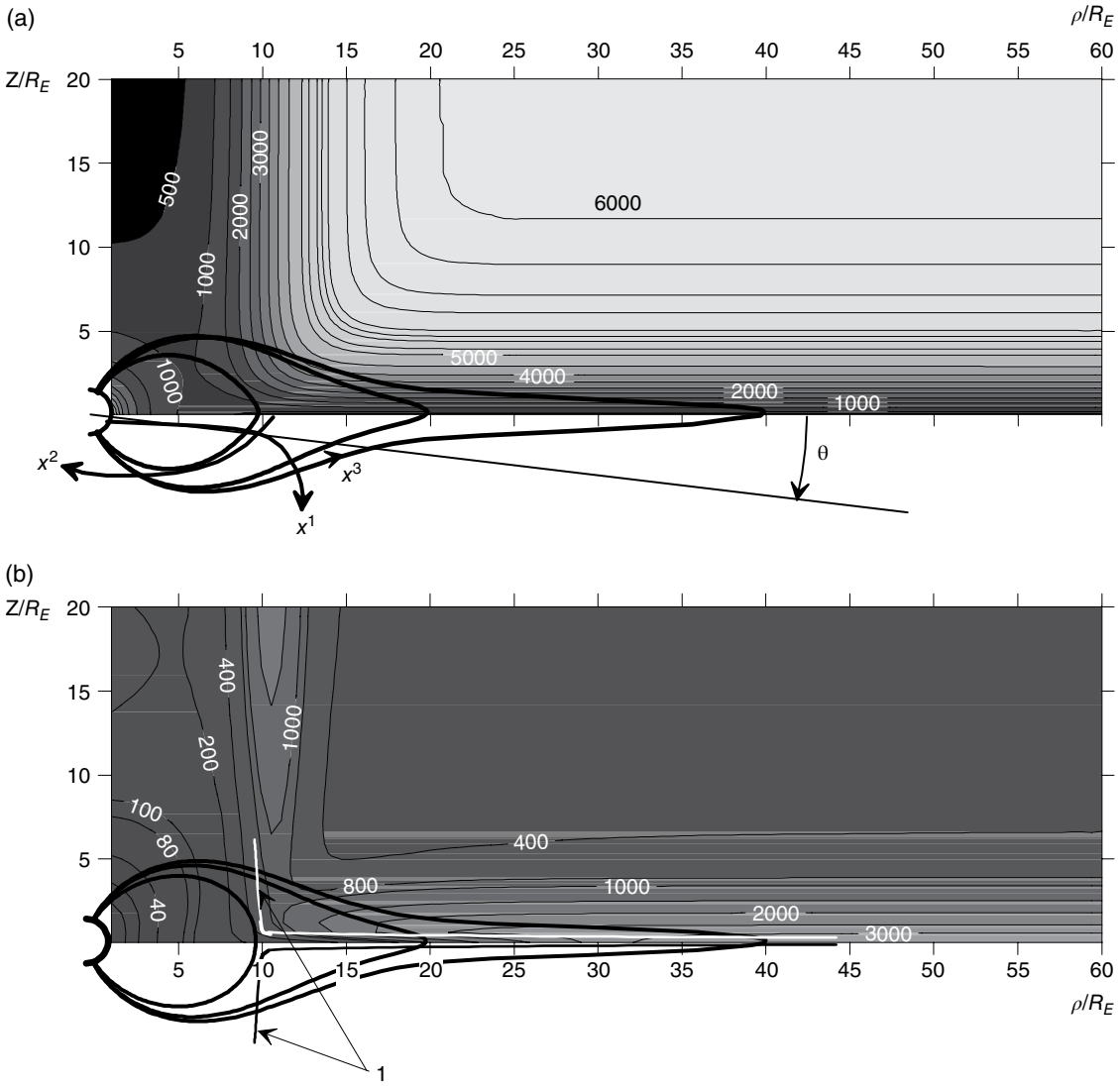

Figure 10.5 Magnetotail model with a current sheet and magnetic field lines for different magnetic shells. (a) Distribution of Alfvén speed v_A(km/s) in the meridional plane and the curvilinear coordinates (x^1, x^2, x^3). (b) SMS speed c_s(km/s) and the shapes of the magnetic field line inflection surfaces (1).

azimuthal angle, then $k_2 \equiv m = 0, 1, 2, 3, \ldots$ is the azimuthal wave number). This model is applicable to oscillations with $m \gg 1$.

In the ideal MHD approximation, the oscillations under study have no field-aligned electric field component. An electric field without field-aligned components can be represented as a decomposition.

$$\mathbf{E} = -\nabla_\perp \varphi + \left[\nabla_\perp \times \Psi\right]$$

where $\nabla_\perp$ is the gradient across magnetic field lines, φ and $\Psi = (0, 0, \psi)$ are, respectively, the scalar and vector potential of the perturbed electric field.

The following equation was obtained in *Leonovich and Kozlov* [2013b] for the scalar electric field potential of the oscillation in question.

$$\hat{L}_S \nabla_1 \hat{L}_T \nabla_1 \varphi - k_2^2 \left(\hat{L}_S \hat{L}_P + \hat{L}_C \right) \varphi = 0 \qquad (10.9)$$

where $\nabla_i \equiv \partial / \partial x^i$ and the following operators in the longitudinal x^3 coordinate are introduced:

$$\hat{L}_T = \frac{1}{\sqrt{g_3}} \nabla_3 \frac{p}{\sqrt{g_3}} \nabla_3 + p \frac{\omega^2}{v_A^2}$$

$$\hat{L}_P = \frac{1}{\sqrt{g_3}} \nabla_3 \frac{p^{-1}}{\sqrt{g_3}} \nabla_3 + p^{-1} \frac{\omega^2}{v_A^2}$$

are the longitudinal toroidal and poloidal operators describing the structure of Alfvén oscillations with toroidal ($m = 0$) and poloidal ($m \to \infty$) polarization in a "cold"

plasma, $p = \sqrt{g_2 / g_1}$, $g = \sqrt{g_1 g_2 g_3}$, where $g_{1,2,3}$ are the metric tensor components;

$$\hat{L}_S = \frac{\varkappa_{1g}\rho_0}{B_0 P_0^\sigma \sqrt{g}} \nabla_3 \frac{\sqrt{g} P_0^\sigma}{g_3 \rho_0} \nabla_3 \frac{B_0}{\varkappa_{1g}} + \frac{\omega^2}{C_s^2}$$

$$\hat{L}_C = \frac{\varkappa_{1g}\omega^2}{v_A^2 \sqrt{g_1 g_2}} \left[\frac{B_0}{\omega^2 P_0^\sigma \sqrt{g_3}} \nabla_3 \frac{\varkappa_{1B} v_A^2 P_0^\sigma}{B_0 \sqrt{g_3}} \nabla_3 - \varkappa_{1P} \right]$$

where P_0 is the plasma pressure, $\sigma = 1/\gamma$, and $\gamma = 5/3$ is the adiabatic index.

During a transition to a homogeneous plasma case, the $\hat{L}_P$ and $\hat{L}_T$ operators produce a dispersion equation for Alfvén waves $\omega^2 = k_\parallel^2 v_A^2$, and the $\hat{L}_S$ operator a dispersion equation for SMS waves $\omega^2 = k_\parallel^2 c_S^2$. Coupling of these waves is described by the $\hat{L}_C$ operator containing logarithmic derivatives of the medium parameters:

$$\varkappa_{1g} = \nabla_1 \left(\ln \sqrt{g_3} \right)$$

$$\varkappa_{1B} = \nabla_1 \left(\ln \sqrt{g_3} B_0 \right), \quad \varkappa_{1P} = \nabla_1 \left(\ln \sqrt{g_3} P_0^\sigma / B_0 \right)$$

Here $g_1^{-1/2} \varkappa_{1g} = -1/R_c$ is the magnetic field line curvature, where R_c is the curvature radius.

The relation between potentials φ and ψ for MHD oscillations with $m \gg 1$ in the main order of perturbation theory has the form

$$ik_2 B_0 \frac{\varkappa_{1g}}{\sqrt{g_3}} \tilde{\Delta}_\perp \psi \approx \nabla_1 B_0 \hat{L}_T \nabla_1 \varphi - k_2^2 B_0 \hat{L}_P \varphi \qquad (10.10)$$

where $\tilde{\Delta}_\perp = g_3 g^{-1/2} \nabla_1 g_2 g^{-1/2} \nabla_1 - k_2^2 g_2^{-1}$. Note that the right side of (10.10) consists of the operators that give a dispersion equation for the Alfvén waves in a homogeneous plasma, $\omega = k_\parallel v_A$. Therefore oscillations of the scalar potential φ can be treated as Alfvén-type oscillations. The left side of (10.10) contains the vector potential component ψ that, in the limit $m \gg 1$, describes the SMS oscillations. In this approximation the ψ potential is proportional to the field line curvature radius, R_c. It has singularities at field line inflection points, where $R_c \to \infty$. In the higher orders of perturbation theory, the oscillation field is regularized at inflection points, but some characteristic peaks will be observed in the distribution of the oscillation amplitude.

Obviously, each of the field lines passing through the current sheet has four such points. Two are located near the current sheet, and the other two in the transition region between the dipole magnetic field and the current sheet magnetic field. The set of such points forms an inflection surface of magnetic field lines. Their cross section in the meridional plane is shown by thin black and white lines in Figure 10.5b.

We can express the oscillation field components in terms of the φ and ψ potentials:

$$E_1 = -\nabla_1 \varphi + ik_2 \frac{g_1}{\sqrt{g}} \psi, \quad E_3 = 0$$

$$E_2 = -ik_2 \varphi - \frac{g_2}{\sqrt{g}} \nabla_1 \psi \qquad (10.11)$$

$$B_1 = \frac{c}{\omega} \frac{g_1}{\sqrt{g}} \nabla_3 \left(k_2 \varphi - i \frac{g_2}{\sqrt{g}} \nabla_1 \psi \right), \qquad B_3 = i \frac{c}{\omega} \tilde{\Delta}_\perp \psi$$

$$B_2 = \frac{c}{\omega} \frac{g_2}{\sqrt{g}} \nabla_3 \left(i \nabla_1 \varphi + k_2 \frac{g_1}{\sqrt{g}} \psi \right) \qquad (10.12)$$

For oscillations with $m \gg 1$, the first term in (10.9) can be neglected near the poloidal resonance surface, in the leading order of perturbation theory, and the remaining equation

$$\hat{L}_S \hat{L}_P \varphi + \hat{L}_C \varphi \approx 0 \qquad (10.13)$$

describes the longitudinal structure of the oscillation field of the coupled modes. Equation (10.13) is a fourth-order equation in the longitudinal x^3 coordinate, describing two oscillation modes, the Alfvén and SMS waves. Accordingly, it has two eigenfrequency sets. Both were studied in *Leonovich and Kozlov* [2013b] in the WKB approximation. The SMS oscillations have lower frequencies and are easily absorbed by the background plasma ions. Therefore we are more interested in the Alfvén oscillation type, which we will consider in accordance with *Leonovich and Kozlov* [2014].

Due to the high conductivity of the ionosphere, these oscillations have the structure of standing waves along geomagnetic field lines. The transverse structure of the main harmonics of these waves is much smaller scale than their longitudinal structure. In this setup, the multiscale method is valid and the scalar potential can be written as $\varphi = U(x^1) H(x^1, x^3)$, where the $U(x^1)$ function describes the small-scale structure of the oscillation field across magnetic shells, and $H(x^1, x^3)$ describes its large-scale structure along magnetic field lines.

Eqaution (10.13) is here the equation for the $H(x^1, x^3)$ function, reducible to the canonical form.

$$\left[\nabla_3^4 + \kappa_3 \nabla_3^3 + \kappa_2 \nabla_3^2 + \kappa_1 \nabla_3 + \kappa_0 \right] H = 0 \qquad (10.14)$$

with rather complicated coefficients κ_i, whose expressions were obtained in *Leonovich and Kozlov* [2014]. Equation (10.14) describes the wave field structure of the coupled modes along geomagnetic field lines. On most

of the stretched magnetic field lines, except a narrow region of the current layer, the first two terms in (10.14) are small compared with the last three (of the order $\beta \ll 1$, where $\beta = 8\pi P_0 / B_0^2$ is the ratio of the gas–kinetic plasma pressure to the magnetic pressure). When solving the problem of the large-scale longitudinal structure of the oscillations, the small terms in (10.14) can be neglected, whereas the remaining terms describe the poloidal Alfvén waves.

However, the $k_2$coefficient varies strongly along the magnetic field line and passes through zero at some points in the current sheet. Near these points small terms with higher derivatives in (10.14) must be taken into account. They describe the interaction between the Alfvén and SMS waves. These points are the special points of equation (10.14). In their vicinity the characteristic scales of Alfvén and SMS waves are the same and a mutual partial linear transformation of these waves takes place. In other words, if an Alfvén wave only is incident away from the transformation point, then the reflection from the transformation region is the sum of the Alfvén and SMS waves. The same happens when the Alfvén wave passes through the transformation point—where the field of the waves passing through this point consists of Alfvén and SMS waves. Unlike resonance points, the oscillation amplitude exhibits no sharp increase near the transformation points.

As a result the total oscillation field on the field lines passing through the current sheet is the sum of the Alfvén and SMS wave fields. Their amplitudes and phases are coupled through the linear transformation mechanism in the current sheet. In the zeroth-order of perturbation theory, the ionosphere can be regarded as a perfectly conductive boundary. Then the boundary conditions on the ionosphere for potential φ are of the form.

$$\varphi\left(x_{\pm}^3\right) = 0, \quad \nabla_3^2\varphi\Big|_{x_{\pm}^3} = \varkappa_{lp}\nabla_3\varphi\Big|_{x_{\pm}^3} \tag{10.15}$$

where $x_{\pm}^3$ are the points where the field line intersects the ionosphere of the Northern and Southern Hemispheres, $\varkappa_{lp} = \nabla_3(\ln p^{-1})$. For the numerical integration of (10.14), we also have to specify the derivatives, $\nabla_3\varphi|_{x_-^3}$ and $\nabla_3^3\varphi|_{x_-^3}$. The first derivative, $\nabla_3\varphi|_{x_-^3}$, defines the total amplitude of the oscillations and can be chosen arbitrarily, but $\nabla_3^3\varphi|_{x_-^3}$ is not determined from any other boundary conditions. Since the boundary conditions (10.15) must be satisfied for either ionosphere, (10.14) must have two free parameters, the eigenvalues for which are to be determined. We will choose the oscillation frequency ω as one such parameter and the derivative $\nabla_3^3\varphi|_{x_-^3}$ as the other.

The solution of (10.14) with boundary conditions (10.15) is a set of standing waves between the magneto-conjugated ionospheres described by a set of $H_N(x^1,\ x^3)$ functions and corresponding eigenfrequencies $\omega = \Omega_N$, where $N = 1, 2, 3, \ldots$ are the wave numbers of longitudinal harmonics. Note that these are not the frequencies of the plasma eigen-oscillations, but they are functions of the transverse coordinate ($\Omega_N \equiv \Omega_N(x^1)$) and determine the structure of the wave field along the magnetic field lines.

Figure 10.6a shows the field-aligned distributions of the main components of the electromagnetic oscillation field calculated numerically for the basic harmonic ($N = 1$). The distributions correspond to the poloidal resonance surface on magnetic shell $L = a / R_E = 15$, where a is the equatorial radius of the field line, R_E is the Earth's radius. The geomagnetic latitude θ as counted from the equatorial plane is used as the longitudinal coordinate (see Figure 10.5a). An interesting feature of the wave field is the SMS-related small-scale structure of the oscillations. This structure manifests itself in the $E_y = E_2 / \sqrt{g_2}$ and $B_x = B_1 / \sqrt{g_1}$ components near the ionosphere only (not shown in the figure) and also in the compressible $B_z = B_3 / \sqrt{g_3}$ component near the equatorial plane, prevailing up to the ionosphere (shown in the separate plot).

A similar spatial structure of coupled oscillations has already been obtained [*Cheremnykh and Parnowski*, 2006; *Mazur et al*., 2014] for some components of the oscillation field. According to our calculations, the SMS-related small-scale structure manifests itself for all oscillation field components near the ionosphere. Moreover, in the distribution of the B_z component, amplitude peaks stand out sharply at the field line inflection points: two near the current sheet and another two in the transition region between the dipole magnetic field and the current sheet field.

The distribution of the basic frequency of the coupled modes and toroidal Alfvén waves over magnetic shells are shown in Figure 10.6c. Note the jumps in the $\Omega_N(x^1)$ distribution in the transition region between the dipole magnetic field and the current sheet field. This is no inaccuracy of numerical calculation. These jumps are due to the following circumstance. Large-scale poloidal Alfvén waves are coupled in the current sheet with different small-scale harmonics of SMS waves having almost the same frequency. The distribution of the eigenfrequencies across magnetic shells has the form of a "bunch" of lines that merge into a single line in the transition layer. Therefore the eigenfrequency quantification technique that we use produces jumps between different oscillation branches in the transition region. They are impossible to avoid. We can only minimize the number of such jumps by selecting proper initial parameters when finding the eigenvalues.

The poloidal oscillation frequency in the current sheet has an imaginary component (growth rate) due to a

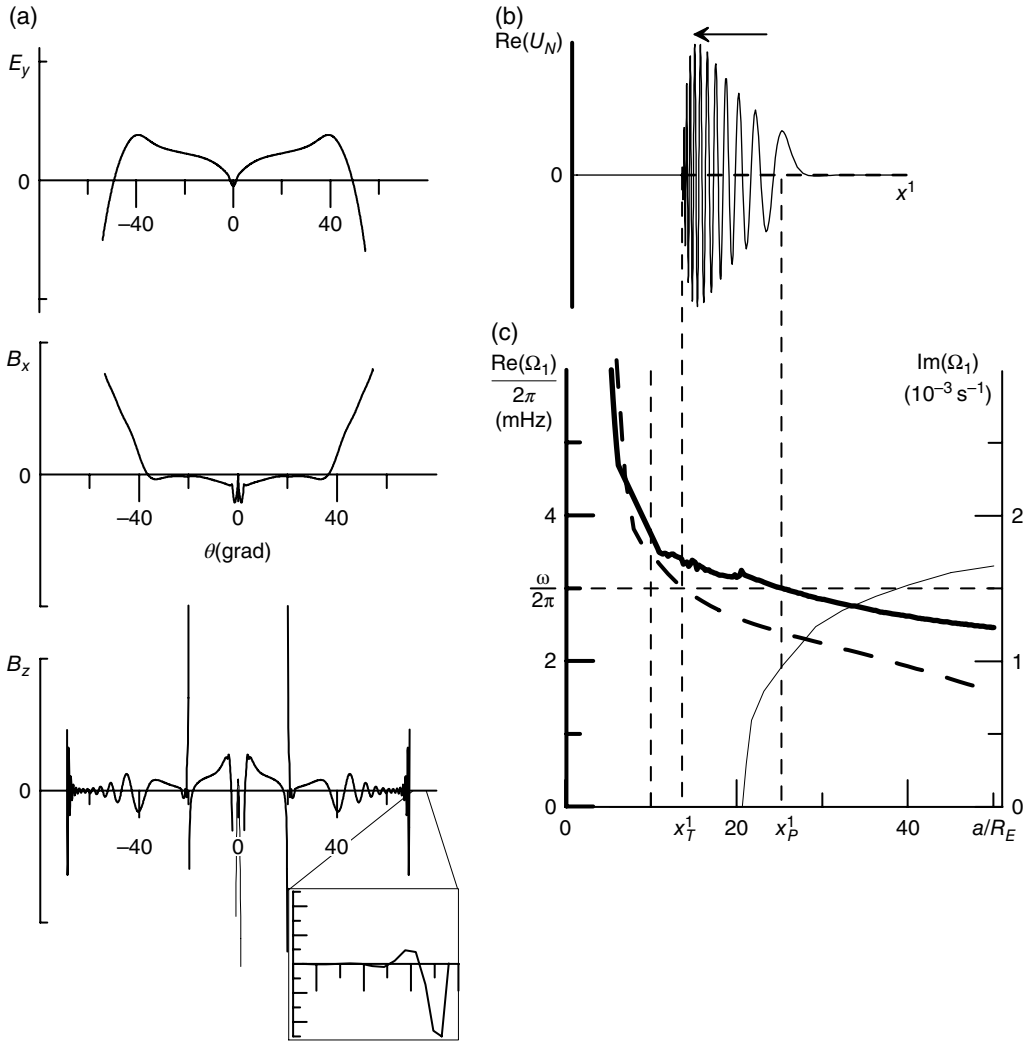

Figure 10.6 (a) Field-aligned distribution of the oscillation electromagnetic field components for the fundamental harmonic of the coupled modes ($N = 1$) on magnetic shell $L = 15$. (b) Structure of the wave field of unstable oscillations between the poloidal $(\xi = 0)$ and toroidal ($\xi = 1$) resonance surfaces. (c) Distribution of the poloidal (thick solid line) and toroidal (dashed line) eigenfrequencies, across magnetic shells, for the basic harmonic of coupled oscillations, and the instability growth rate (thin solid line).

ballooning instability. Note that this instability is not a consequence of Alfvén and SMS wave coupling. It also appears in uncoupled oscillations [*Leonovich and Kozlov*, 2013b]. In this problem we ignore the fact that SMS waves decay strongly in the magnetosphere due to their interaction with background plasma ions [*Leonovich and Kozlov*, 2009]. If this damping is included, the coupled mode can, conversely, become damped.

In the direction across magnetic shells, the transparency region for monochromatic waves with frequency ω is located between the poloidal $\left(x_P^1\right)$ and toroidal $\left(x_T^1\right)$ resonance surfaces (see Figure 10.6c). We have to use the full form of (10.9) to describe the oscillation structure across magnetic shells. After a special integration procedure of (10.9) along the field line involving the boundary conditions that take into account the finite conductivity of and the presence of external currents in the ionosphere [*Leonovich and Mazur*, 1996] and linearizing the coefficients near the poloidal resonance surface, we obtain the equation

$$\frac{\partial^2}{\partial \xi^2} U_N + (\xi + i\varepsilon_N) U_N = \frac{a^{2/3}}{k_y^{4/3}} I_{\|N} \qquad (10.16)$$

describing the small-scale structure of the coupled modes across magnetic shells near the poloidal resonance surface. Here $\xi = (x^1 - x_P^1)/\Delta$, where $\Delta = a^{1/3}/k_y^{2/3}$, a is the characteristic scale of $\Omega_N(x^1)$ near the poloidal surface, $k_y \sim k_2$, $\varepsilon_N = 2(\gamma_N - \delta_N)(k_y a)^{2/3}/\omega$, δ_N is the ballooning

instability growth rate, γ_N is the decrement due to the finite ionospheric conductivity, $I_{\|N}$ is the oscillation source determined by external currents in the ionosphere.

If the localization scale of source $I_{\|N}$ is much larger than the localization scale of the oscillations, the right-hand side in (10.16) can be assumed constant, and the solution has the form

$$U_N\left(x^1\right) = \frac{a_N^{2/3}}{k_y^{4/3}} I_{\|N} \mathrm{Gi}\left(\xi + i\varepsilon_N\right)$$

where the Gi(z) function is the solution of an inhomogeneous Airy equation decreasing into the opacity region like z^{-1}.

The total structure of the unstable oscillations ($\varepsilon_N < 0$) across magnetic shells is shown in Figure 10.6b. The wave is excited at the poloidal resonance surface by external currents in the ionosphere and moves away from it toward the toroidal surface. The amplitude of the oscillations increases due to the ballooning instability, but near the toroidal resonance surface the oscillations are completely absorbed due to their dissipation in the ionosphere.

Thus we can use the following features in the spatial structure of these coupled modes on closed magnetic field lines to identify them. Since these oscillations are standing waves along magnetic field lines, the phase shift between their $E_y = E_2 / \sqrt{g_2}$ and $B_x = B_1 / \sqrt{g_1}$ components is $\pi/2$, as follows from (10.10). If we do not take into account possible small-scale oscillations near the ionosphere, the transverse B_x, B_y and E_x, E_y components of the electromagnetic field are large scale for the basic harmonics of standing waves, while the $B_z = B_3 / \sqrt{g_3}$ field-aligned component is small scale, along the field line.

In the opacity region along the radial x^1 coordinate and near the poloidal resonance surface ($x^1 = x_P^1$), the phase shift between the $B_x = B_1 / \sqrt{g_1}$ and $B_y = B_2 / \sqrt{g_2}$ components is also $\pi/2$, which corresponds to a standing wave over x^1. However, in the transparency region ($x_P^1 < x^1 < x_T^1$) away from the poloidal resonance surface and closer to the toroidal one, the phase shift between these components changes gradually to π, which is typical of a running wave along the radial coordinate. If the oscillations are unstable, the amplitudes of all components first increase and then decrease toward the toroidal surface. The polarization of the oscillations changes from poloidal (with dominant B_x and E_y components) to toroidal (with dominant B_y and E_x components).

And finally, sharp narrowly localized peaks in the oscillation amplitude distribution should be observed at points where the field line crosses the inflection surfaces, especially noticeable in the B_z component distribution. Two such peaks are located at the current sheet boundaries, and the two others in the region where the field line crosses the transition region between the dipole magnetic field and current sheet field.

10.5. FLAPPING OSCILLATIONS OF THE CURRENT SHEET

Last, let us address the recently discovered kink-like oscillations of the magnetotail current sheet [*Zhang et al.*, 2002]. These oscillations differ fundamentally from eigen MHD oscillations that propagate in the current sheet without changing its configuration [*Fruit et al.*, 2009; *Wright and Allan*, 2008; *Dmitrienko*, 2013]. On the contrary, the discovered kink-like oscillations are oscillations of the current sheet itself, similar to a piece of fabric fluttering in the wind. In this regard they are called "flapping modes".

Flapping modes are detected in *in situ* observations as the spacecraft is repeatedly crossed by the current sheet [*Zhang et al.*, 2002]. A statistical study in *Sergeev et al.* [2006] shows that their occurrence increases sharply with distance from the Earth, reaching a maximum in the middle tail. Flapping modes are often observed during the substorm expansion phase. The average frequency of these oscillations is ~ 0.035 s^{-1}, their wavelength is 2–5 R_E, their group velocity is $\sim 30-70$ km / s, and their vertical oscillation amplitude reaches 2–3 R_E [*Runov et al.*, 2009].

Several theoretical interpretations have been set forth to explain the observed flapping modes. In *Golovchanskaya and Maltsev* [2005], the flapping modes are regarded as unstable "ballooning modes" (i.e., essentially, as coupled poloidal Alfvén and SMS waves). Based on an analysis of the local dispersion relations in *Ohtani et al.* [1989] and *Liu* [1997], it was shown that the group velocity of these waves along the current sheet, $\sim 40-400$ km / s, is equal to the velocity of the observed flapping modes. Oscillations that are antisymmetric relative to the equilibrium position of the current sheet are considered as flapping modes. In particular, they can be observed as kink-like oscillations, unlike the symmetrical sausage modes. It should be noted, however, that, as follows from the findings in the previous section, the typical oscillation wavelengths along the current sheet $\lambda_x \sim \Delta_N / m$ (where $\Delta_N = \left|x_{TN}^1 - x_{PN}^1\right|$, $m \gg 1$) are much smaller than the observed ones $\lambda_x \sim \Delta_N$.

In *Zelenyi et al.* [2009], observed flapping modes are explained as eigen-drift modes in a thin current sheet. They can be unstable like tearing modes. These modes differ by the direction of their wave vector. In drift modes, the wave vector is directed perpendicular to the plasma motion direction, while in tearing modes, it is parallel. It was noted that oscillations with any intermediate directions of the wave vectors can be unstable.

The following concept of flapping modes was developed in *Erkaev et al.* [2009]. It was suggested that oscillations with the observed frequencies and propagation velocities could be a signature of an original mode of MHD oscillations due to different gradients of the

background magnetic field components $\nabla_z B_x$ and $\nabla_x B_z$. For a linear mode of the form $\exp(i\omega t - ik_y y)$, the oscillation frequency is $\omega = \sqrt{\Delta L_x \nabla_z B_x \nabla_x B_z / 4\pi\rho_0}$, where Δ is the typical current sheet thickness and L_x is the typical scale of $B_z(x/L_x)$. For the typical values of the medium parameters $B_x \approx 20$ nT, $B_z \approx 2$ nT, $\Delta \approx R_E$, $L_x \sim 5R_E$, $k_y\Delta \sim 0.7$, and $\nabla_z B_x \sim B_z / L_x$, the following estimates were obtained for the frequency and group velocity of the oscillations in question: $\omega \sim 0.03\ \mathrm{s}^{-1}$, $v_g \sim 60$ km/s, coinciding with the observed values for flapping modes.

Let us note the disadvantages of all the flapping oscillation concept proposed above. All the above papers considered the flapping oscillation development in a linear local approximation. In other words, all the MHD oscillations proposed for the flapping modes are considered as small-amplitude oscillations against an almost constant background. However, it is clear that the current sheet fluctuations with amplitudes $2-3R_E$ cannot be regarded as small fluctuations. In all concepts proposed above the magnetotail is not considered as a single object. It seems natural that the current sheet fluctuations are associated with the fluctuations of the magnetotail in the solar wind flow. To be sure, an adequate nonlinear theory of the magnetotail instability in the solar wind flow is still absent. Nevertheless, there are numerous MHD simulations showing exactly this magnetotail behavior in the high-speed solar wind flows. This suggests that we may hope to see an adequate theory of this phenomenon developed in the near future.

10.6. SUMMARY

Let us list the main results of this chapter based on the reviewed observational data and theoretical models of MHD oscillations in the magnetotail:

1. The processes under scrutiny are those involving FMS wave penetration from the solar wind into the magnetosphere and the amplification of MHD oscillations excited at the magnetopause under the effect of the Kelvin–Helmholtz instability. It is shown that in the low-frequency part of the spectrum, covering the geomagnetic Pc5 pulsation range and below, oscillations with large field-aligned wavelengths $k_\parallel \lesssim r_m^{-1}$, where $r_m \approx 20-30R_E$ is the magnetopause radius, can enter into an unstable regime.

Most FMS waves penetrating into the magnetosphere have resonance surfaces in the magnetopause transition layer. Intense interaction takes place between the magnetosonic oscillations and the background plasma ions at the resonance shells for SMS waves. As a result the waves are damped, and the ions acquire additional momentum and energy. It is shown that the FMS wave flux from the magnetosheath into the magnetosphere can form Earthward plasma flows with velocities of 50–150 km/s. Periods of a long-lasting Northern IMF component show no momentum transfer from the solar wind into the magnetosphere due to a magnetic field reconnection at the dayside magnetopause. Observations in the high-latitude ionosphere show that cells with reverse plasma convection form in the magnetotail areas adjacent to the magnetopause over the same periods. Formation of these cells can be explained by a mechanism for a wave transfer of the momentum from the solar wind into the magnetosphere.

2. The problem is solved about the eigen-oscillation structure and spectrum for the FMS resonator in the near-Earth part of the magnetotail plasma sheet. It is shown that such a resonator is formed in periods of low enough geomagnetic disturbance, $K_P \sim 1$. The resonator eigenfrequencies are not distributed randomly but are grouped into separate clusters. The mean frequencies in each of such clusters are close to one of the "magic frequencies" and cover the whole set of the observed ULF waves with a discrete spectrum.

3. Coupled Alfvén and SMS oscillations are studied on the tailward-stretched closed magnetic field lines passing through the current sheet. It is shown that coupling of the modes occurs in the current sheet at the resonance surfaces for poloidal Alfvén waves and takes the form of their partial linear transformation into SMS waves. Under certain conditions, these coupled oscillations become unstable due to the action of a "ballooning" instability caused by magnetic field line curvature and the plasma pressure gradient directed along the curvature radius. This instability is regarded as one of the possible trigger mechanisms for geomagnetic field line reconnection in the near-Earth part of the current sheet during magnetospheric substorms. Across the magnetic shells, the coupled mode has the form of a wave running from the poloidal to the toroidal resonance surface for Alfvén waves.

4. The main theoretical concepts proposed for interpreting the recently discovered "flapping" oscillations of the magnetotail current sheet are discussed. These oscillations have many interpretations in the current theoretical concepts: as coupled "ballooning" modes, as "drift" modes in a thin current sheet, as specific MHD modes due to the different gradients in the geomagnetic field components. All these concepts are based on theoretical approaches studying linear oscillations of small amplitude developing in a stable background plasma. However, it appears that these oscillations should be considered as strongly nonlinear current sheet oscillations occurring together with the magnetotail oscillations in the solar wind flow. An adequate theory on this phenomenon can be expected to be developed over the next decade.

ACKNOWLEDGMENT

This work was supported by the Grant of the Russian Scientific Foundation (Project No. 14-37-00027).

REFERENCES

Agapitov, O., K.-H. Glassmeier, F. Plaschke, H.-U. Auster, D. Constantinescu, V. Angelopoulos, W. Magnes, R. Nakamura, C. W. Carlson, S. Frey, and J. P. McFadden (2009), Surface waves and field line resonances: A THEMIS case study, *J. Geophys. Res.*, *114*, A00C27, doi:10.1029/2008JA013553.

Agapitov, O. V., and O. K. Cheremnykh (2013), Magnetospheric ULF waves driven by external sources, *Adv. Astron. Space Phys.*, *3*, 12–19.

Akhiezer, A. I., I. A. Akhiezer, R. V. Polovin, A. G. Sitenko, and K. N. Stepanov (1975), *Plasma Electrodynamics, Vol. 1: Linear Theory, Vol. 2: Non-linear Theory and Fluctuations*, Oxford Pergamon Press International Series on Natural Philosophy. Oxford University Press.

Allan, W., and E. M. Poulter (1992), ULF waves—Their relationship to the structure of the Earth's magnetosphere, *Rep. Prog. Phys.*, *55*, 533–598, doi:10.1088/0034-4885/55/5/001.

Allan, W., and A. N. Wright (1998), Hydromagnetic wave propagation and coupling in a magnetotail waveguide, *J. Geophys. Res.*, *103*, 2359–2368, doi:10.1029/97JA02874.

Archer, M. O., M. D. Hartinger, and T. S. Horbury (2013), Magnetospheric "magic" frequencies as magnetopause surface eigenmodes, *Geophys. Res. Lett.*, *40*, 5003–5008, doi:10.1002/grl.50979.

Cao, J. B., X. H. Wei, A. Y. Duan, H. S. Fu, T. L. Zhang, H. Reme, and I. Dandouras (2013), Slow magnetosonic waves detected in reconnection diffusion region in the Earth's magnetotail, *J. Geophys. Res.*, *118*, 1659–1666, doi:10.1002/jgra.50246.

Chen, L., and A. Hasegawa (1974), A theory of long-period magnetic pulsations: 1. Steady state excitation of field line resonance, *J. Geophys. Res.*, *79*, 1024–1032, doi:10.1029/JA079i007p01024.

Cheng, C. Z. (2004), Physics of substorm growth phase, onset, and dipolarization, *Space Sci. Rev*., *113*, 207–270, doi:10.1023/B:SPAC.0000042943.59976.0e.

Cheng, C. Z., and A. T. Y. Lui (1998), Kinetic ballooning instability for substorm onset and current disruption observed by AMPTE/CCE, *Geophys. Res. Lett.*, *25*, 4091–4094, doi:10.1029/1998GL900093.

Cheremnykh, O. K., and A. S. Parnowski (2006), Influence of ionospheric conductivity on the ballooning modes in the inner magnetosphere of the Earth, *Adv. Space Res.*, *37*, 599–603, doi:10.1016/j.asr.2005.01.073.

Dmitrienko, I. S. (2013), Evolution of FMS and Alfvén waves produced by the initial disturbance in the FMS waveguide, *J. Plasma Phys.*, *79*, 7–17, doi:10.1017/S0022377812000608.

Du, J., T. L. Zhang, R. Nakamura, C. Wang, W. Baumjohann, A. M. Du, M. Volwerk, K.-H. Glassmeier, and J. P. McFadden (2011), Mode conversion between Alfvén and slow waves observed in the magnetotail by THEMIS, *Geophys. Res. Lett.*, *38*, L07101, doi:10.1029/2011GL046989.

ErdéLyi, R., and Y. Taroyan (2003), On resonantly excited MHD waves in the magnetotail, *J. Geophys. Res.*, *108*, 1043, doi:10.1029/2002JA009586.

Erkaev, N. V., V. S. Semenov, I. V. Kubyshkin, M. V. Kubyshkina, and H. K. Biernat (2009), MHD model of the flapping motions in the magnetotail current sheet, *J. Geophys. Res.*, *114*, A03206, doi:10.1029/2008JA013728.

Förster, M., S. E. Haaland, G. Paschmann, J. M. Quinn, R. B. Torbert, H. Vaith, and C. A. Kletzing (2008), High-latitude plasma convection during Northward IMF as derived from in-situ magnetospheric Cluster EDI measurements, *Ann. Geophys.*, *26*, 2685–2700, doi:10.5194/angeo-26-2685-2008.

Foullon, C., C. J. Farrugia, A. N. Fazakerley, C. J. Owen, F. T. Gratton, and R. B. Torbert (2008), Evolution of Kelvin–Helmholtz activity on the dusk flank magnetopause, *J. Geophys. Res.*, *113*, A11203, doi:10.1029/2008JA013175.

Fruit, G., P. Louarn, A. Tur, and D. Le QuéAu (2002), On the propagation of magnetohydrodynamic perturbations in a Harris-type current sheet: 1. Propagation on discrete modes and signal reconstruction, *J. Geophys. Res*., *107*, 1411, doi:10.1029/2001JA009212.

Fujita, S., K. H. Glassmeier, and K. Kamide (1996), MHD waves generated by the Kelvin-Helmholtz instability in a nonuniform magnetosphere, *J. Geophys. Res.*, *101*, 27,317–27,326, doi:10.1029/96JA02676.

Golovchanskaya, I. V., and Y. P. Maltsev (2005), On the identification of plasma sheet flapping waves observed by Cluster, *Geophys. Res. Lett.*, *32*, L02102, doi:10.1029/2004GL021552.

Hameiri, E., P. Laurence, and M. Mond (1991), The ballooning instability in space plasmas, *J. Geophys. Res.*, *96*, 1513–1526, doi:10.1029/90JA02100.

Hartinger, M., V. Angelopoulos, M. B. Moldwin, K.-H. Glassmeier, and Y. Nishimura (2011), Global energy transfer during a magnetospheric field line resonance, *Geophys. Res. Lett.*, *38*, L12101, doi:10.1029/2011GL047846.

Hasegawa, H., M. Fujimoto, K. Takagi, Y. Saito, T. Mukai, and H. RèMe (2006), Single-spacecraft detection of rolled-up Kelvin–Helmholtz vortices at the flank magnetopause, *J. Geophys. Res.*, *111*, A09203, doi:10.1029/2006JA011728.

Hughes, W. J. (1994), Magnetospheric ULF waves: A tutorial with a historical perspective, Washington DC: *AGU Geophys. Monogr. Ser*., *81*, 1–11, doi:10.1029/GM081p0001.

Kangas, J., A. Guglielmi, and O. Pokhotelov (1998), Morphology and physics of short-period magnetic pulsations, *Space Sci. Rev*., *83*, 435–512.

Keiling, A. (2009), Alfvén Wwaves and their roles in the dynamics of the Earth's magnetotail: A review, *Space Sci. Rev*., *142*, 73–156, doi:10.1007/s11214-008-9463-8.

Keiling, A. (2012), Pi2 pulsations driven by ballooning instability, *J. Geophys. Res.*, *117*, A03228, doi:10.1029/2011JA017223.

Kepko, L., H. E. Spence, and H. J. Singer (2002), ULF waves in the solar wind as direct drivers of magnetospheric pulsations, *Geophys. Res. Lett.*, *29*, 1197, doi:10.1029/2001GL014405.

Klimushkin, D. Y., P. N. Mager, and V. A. Pilipenko (2012), On the ballooning instability of the coupled Alfvén and drift compressional modes, *Earth Planet. Space*, *64*, 777–781, doi:10.5047/eps.2012.04.002.

Kozlov, D. A., A. S. Leonovich, and J. B. Cao (2006), The structure of standing Alfvén waves in a dipole magnetosphere with moving plasma, *Ann. Geophys.*, *24*, 263–274, doi:10.5194/angeo-24-263-2006.

Kozlov, D. A., N. G. Mazur, V. A. Pilipenko, and E. N. Fedorov (2014), Dispersion equation for ballooning modes

in two-component plasma, *J. Plasma Phys.*, *80*, 379–393, doi:10.1017/S0022377813001347.

Lee, D.-H., and R. L. Lysak (1999), MHD waves in a three-dimensional dipolar magnetic field: A search for Pi2 pulsations, *J. Geophys. Res.*,*104*,28,691–28,700,doi:10.1029/1999JA900377.

Leonovich, A. S. (2001), A theory of field line resonance in a dipole-like axisymmetric magnetosphere, *J. Geophys. Res.*, *106*, 25,803–25,812, doi:10.1029/2001JA000104.

Leonovich, A. S. (2011a), MHD-instability of the magnetotail: Global modes, *Planet. Space Sci.*, *59*, 402–411, doi:10.1016/j.pss.2011.01.006.

Leonovich, A. S. (2011b), A theory of MHD instability of an inhomogeneous plasma jet, *J. Plasma Phys.*, *77*, 315–337, doi:10.1017/S0022377810000346.

Leonovich, A. S. (2012), Wave mechanism of the magnetospheric convection, *Planet. Space Sci.*, *65*, 67–75, doi:10.1016/j.pss.2012.01.009.

Leonovich, A. S., and D. A. Kozlov (2009), Alfvénic and magnetosonic resonances in a nonisothermal plasma, *Plasma Phys. Control. Fus.*, *51*(8), 085,007, doi:10.1088/0741-3335/51/8/085007.

Leonovich, A. S., and D. A. Kozlov (2013a), Magnetosonic resonances in the magnetospheric plasma, *Earth Planet. Space*, *65*, 369–384, doi:10.5047/eps.2012.07.002.

Leonovich, A. S., and D. A. Kozlov (2013b), On ballooning instability in current sheets, *Plasma Phys. Control. Fus.*, *55*(8), 085013, doi:10.1088/0741-3335/55/8/085013.

Leonovich, A. S., and D. A. Kozlov (2014), Coupled guided modes in the magnetotails: Spatial structure and ballooning instability, *Astrophys. Space Sci.*, *353*, 9–23, doi:10.1007/s10509-014-1999-3.

Leonovich, A. S., and V. A. Mazur (1990), The spatial structure of poloidal Alfvén oscillations of an axisymmetric magnetosphere, *Planet. Space Sci.*, *38*, 1231–1241, doi:10.1016/0032-0633(90)90128-D.

Leonovich, A. S., and V. A. Mazur (1993), A theory of transverse small-scale standing Alfvén waves in an axially symmetric magnetosphere, *Planet. Space Sci.*, *41*, 697–717, doi:10.1016/0032-0633(93)90055-7.

Leonovich, A. S., and V. A. Mazur (1995), Magnetospheric resonator for transverse-small-scale standing Alfvén waves, *Planet. Space Sci.*, *43*, 881–883, doi:10.1016/0032-0633(94)00206-7.

Leonovich, A. S., and V. A. Mazur (1996), Penetration to the Earthś surface of standing Alfvén waves excited by external currents in the ionosphere, *Ann. Geophys.*, *14*, 545–556, doi:10.1007/s00585-996-0545-1.

Leonovich, A. S., and V. A. Mazur (2000), Structure of magnetosonic eigenoscillations of an axisymmetric magnetosphere, *J. Geophys. Res.*, *105*, 27,707–27,716, doi:10.1029/2000JA900108.

Leonovich, A. S., and V. A. Mazur (2005), Why do ultra-low-frequency MHD oscillations with a discrete spectrum exist in the magnetosphere? *Ann. Geophys.*, *23*, 1075–1079, doi:10.5194/angeo-23-1075-2005.

Leonovich, A. S., and V. A. Mazur (2008), Eigen ultra-low-frequency magnetosonic oscillations of the near plasma sheet, *Cosm. Res.*, *46*, 327–334, doi:10.1134/S0010952508040072.

Leonovich, A. S., and V. V. Mishin (2005), Stability of magnetohydrodynamic shear flows with and without bounding walls, *J. Plasma Phys.*, *71*, 645–664, doi:10.1017/S002237780400337X.

Liu, W. W. (1997), Physics of the explosive growth phase: Ballooning instability revisited, *J. Geophys. Res.*, *102*, 4927–4931, doi:10.1029/96JA03561.

Lysak, R. L., Y. Song, and T. W. Jones (2009), Propagation of Alfvén waves in the magnetotail during substorms, *Ann. Geophys.*, *27*, 2237–2246, doi:10.5194/angeo-27-2237-2009.

Mager, P. N., D. Y. Klimushkin, V. A. Pilipenko, and S. Schäfer (2009), Field-aligned structure of poloidal Alfvén waves in a finite pressure plasma, *Ann. Geophys.*, *27*, 3875–3882, doi:10.5194/angeo-27-3875-2009.

Mann, I. R., A. N. Wright, K. J. Mills, and V. M. Nakariakov (1999), Excitation of magnetospheric waveguide modes by magnetosheath flows, *J. Geophys. Res.*, *104*, 333–354, doi:10.1029/1998JA900026.

Mazur, N. G., E. N. Fedorov, and V. A. Pilipenko (2013), Ballooning modes and their stability in a near-Earth plasma, *Earth Planet. Space*, *65*, 463–471, doi:10.5047/eps.2012.07.006.

Mazur, N. G., E. N. Fedorov, and V. A. Pilipenko (2014), Longitudinal structure of ballooning MHD disturbances in a model magnetosphere, *Cosm. Res.*, *52*, 175–184, doi:10.1134/S0010952514030071.

Mazur, V. A. (2010), Resonance excitation of the magnetosphere by hydromagnetic waves incident from solar wind, *Plasma Phys. Rep.*, *36*, 953–963, doi:10.1134/S1063780X10110048.

Mazur, V. A., and D. A. Chuiko (2011), Excitation of a magnetospheric MHD cavity by Kelvin–Helmholtz instability, *Plasma Phys. Rep.*, *37*, 913–934, doi:10.1134/S1063780X11090121.

Mazur, V. A., and D. A. Chuiko (2013), Influence of the outer magnetospheric magnetohydrodynamic waveguide on the reflection of hydromagnetic waves from a shear flow at the magnetopause, *Plasma Phys. Rep.*, *39*, 959–975, doi:10.1134/S1063780X13120064.

Mazur, V. A., and A. S. Leonovich (2006), ULF hydromagnetic oscillations with the discrete spectrum as eigenmodes of MHD-resonator in the near-Earth part of the plasma sheet, *Ann. Geophys.*, *24*, 1639–1648, doi:10.5194/angeo-24-1639-2006.

McKenzie, J. F. (1970), Hydromagnetic wave interaction with the magnetopause and the bow shock, *Planet. Space Sci.*, *18*, 1–23, doi:10.1016/0032-0633(70)90063-2.

Mishin, V. V. (1981), On the MHD instability of the earth's magnetopause and its geophysical effects, *Planet. Space Sci.*, *29*, 359–363, doi:10.1016/0032-0633(81)90024-6.

Miura, A. (1992), Kelvin–Helmholtz instability at the magnetospheric boundary—Dependence on the magnetosheath sonic Mach number, *J. Geophys. Res.*, *97*, 10,655, doi:10.1029/92JA00791.

Miura, A., and P. L. Pritchett (1982), Nonlocal stability analysis of the MHD Kelvin–Helmholtz instability in a compressible plasma, *J. Geophys. Res.*, *87*, 7431–7444, doi:10.1029/JA087iA09p07431.

Ohtani, S., A. Miura, and T. Tamao (1989), Coupling between Alfvén and slow magnetosonic waves in an inhomogeneous finite-beta plasma, I: Coupled equations and physical

mechanism, II: Eigenmode analysis of localized ballooning-interchange instability, *Planet. Space Sci.*, *37*, 567–577, doi: 10.1016/0032-0633(89)90097-4.

Pilipenko, V. A. (1990), ULF waves on the ground and in space, *J. Atm. Ter. Phys.*, *52*, 1193–1209.

Plaschke, F., K.-H. Glassmeier, H. U. Auster, O. D. Constantinescu, W. Magnes, V. Angelopoulos, D. G. Sibeck, and J. P. McFadden (2009), Standing Alfvén waves at the magnetopause, *Geophys. Res. Lett.*, *36*, L02104, doi:10.1029/2008GL036411.

Potapov, A. S., T. N. Polyushkina, and V. A. Pulyaev (2013), Observations of ULF waves in the solar corona and in the solar wind at the Earth's orbit, *J. Atm. Solar-Ter. Phys.*, *102*, 235–242, doi:10.1016/j.jastp.2013.06.001.

Radoski, H. R. (1974), A theory of latitude dependent geomagnetic micropulsations: The asymptotic fields, *J. Geophys. Res.*, *79*, 595–603, doi:10.1029/JA079i004p00595.

Rankin, R., F. Fenrich, and V. T. Tikhonchuk (2000), Shear Alfvén waves on stretched magnetic field lines near midnight in Earth's magnetosphere, *Geophys. Res. Lett.*, *27*, 3265–3268, doi:10.1029/2000GL000029.

Rankin, R., K. Kabin, and R. Marchand (2006), Alfvénic field line resonances in arbitrary magnetic field topology, *Adv. Space Res.*, *38*, 1720–1729, doi:10.1016/j.asr.2005.09.034.

Runov, A., V. Angelopoulos, V. A. Sergeev, K.-H. Glassmeier, U. Auster, J. McFadden, D. Larson, and I. Mann (2009), Global properties of magnetotail current sheet flapping: THEMIS perspectives, *Ann. Geophys.*, *27*, 319–328, doi:10.5194/angeo-27-319-2009.

Ruohoniemi, J. M., R. A. Greenwald, K. B. Baker, and J. C. Samson (1991), HF radar observations of Pc5 field line resonances in the midnight/early morning MLT sector, *J. Geophys. Res.*, *96*, 15,697, doi:10.1029/91JA00795.

Saito, M. H., Y. Miyashita, M. Fujimoto, I. Shinohara, Y. Saito, and T. Mukai (2008), Modes and characteristics of low-frequency MHD waves in the near-Earth magnetotail prior to dipolarization: Fitting method, *J. Geophys. Res.*, *113*, A06201, doi:10.1029/2007JA012778.

Saka, O., K. Hayashi, and M. Thomsen (2014), Pre-onset auroral signatures and subsequent development of substorm auroras: a development of ionospheric loop currents at the onset latitudes, *Ann. Geophys.*, *32*, 1011–1023, doi:10.5194/angeo-32-1011-2014.

Samson, J. C., and R. Rankin (1994), The coupling of solar wind energy to MHD cavity modes, waveguide modes, and field line resonances in the Earth's magnetosphere, *AGU Geophys. Monogr. Ser.*, *81*, 253–264, doi:10.1029/GM081p0253.

Samson, J. C., B. G. Harrold, J. M. Ruohoniemi, R. A. Greenwald, and A. D. M. Walker (1992), Field line resonances associated with MHD waveguides in the magnetosphere, *Geophys. Res. Lett.*, *19*, 441–444, doi:10.1029/92GL00116.

Sarris, T. E., W. Liu, K. Kabin, X. Li, S. R. Elkington, R. Ergun, R. Rankin, V. Angelopoulos, J. Bonnell, K. H. Glassmeier, and U. Auster (2009), Characterization of ULF pulsations by THEMIS, *Geophys. Res. Lett.*, *36*, L04104, doi:10.1029/2008GL036732.

Sergeev, V. A., R. J. Pellinen, and T. I. Pulkkinen (1996), Steady magnetospheric convection: A review of recent results, *Space Sci. Rev.*, *75*, 551–604, doi:10.1007/BF00833344.

Sergeev, V. A., D. A. Sormakov, S. V. Apatenkov, W. Baumjohann, R. Nakamura, A. V. Runov, T. Mukai, and T. Nagai (2006), Survey of large-amplitude flapping motions in the midtail current sheet, *Ann. Geophys.*, *24*, 2015–2024, doi:10.5194/angeo-24-2015-2006.

Southwood, D. J. (1974), Some features of field line resonances in the magnetosphere, *Planet. Space Sci.*, *22*, 483–491, doi:10.1016/0032-0633(74)90078-6.

Southwood, D. J., and W. J. Hughes (1983), Theory of hydromagnetic waves in the magnetosphere, *Space Sci. Rev.*, *35*, 301–366, doi:10.1007/BF00169231.

Southwood, D. J., and M. A. Saunders (1985), Curvature coupling of slow and Alfvén MHD waves in a magnetotail field configuration, *Planet. Space Sci.*, *33*, 127–134, doi:10.1016/0032-0633(85)90149-7.

Stasiewicz, K., P. Bellan, C. Chaston, C. Kletzing, R. Lysak, J. Maggs, O. Pokhotelov, C. Seyler, P. Shukla, L. Stenflo, A. Streltsov, and J.-E. Wahlund (2000), Small scale Alfvénic structure in the aurora, *Space Sci. Rev.*, *92*, 423–533.

Takahashi, K., K.-H. Glassmeier, V. Angelopoulos, J. Bonnell, Y. Nishimura, H. J. Singer, and C. T. Russell (2011), Multisatellite observations of a giant pulsation event, *J. Geophys. Res.*, *116*, A11223, doi:10.1029/2011JA016955.

Tamao, T. (1965), Transmission and coupling resonance of hydromagnetic disturbances in the non-uniform Earth's magnetosphere, *Sci. Rep. Tohoku Univ.*, *17*, 43–54.

Turkakin, H., R. Rankin, and I. R. Mann (2013), Primary and secondary compressible Kelvin–Helmholtz surface wave instabilities on the Earth's magnetopause, *J. Geophys. Res.*, *118*, 4161–4175, doi:10.1002/jgra.50394.

Turkakin, H., I. R. Mann, and R. Rankin (2014), Kelvin–Helmholtz unstable magnetotail flow channels: Deceleration and radiation of MHD waves, *Geophys. Res. Lett.*, *41*, 3691–3697, doi:10.1002/2014GL060450.

Viall, N. M., L. Kepko, and H. E. Spence (2009), Relative occurrence rates and connection of discrete frequency oscillations in the solar wind density and dayside magnetosphere, *J. Geophys. Res.*, *114*, A01201, doi:10.1029/2008JA013334.

Villante, U. (2007), *Ultra Low Frequency Waves in the Magnetosphere*, In: Handbook of the Solar-Terrestrial Environment Kamide, Y. and A.~C.-L. Chian (eds.), Springer, Netherlands, p. 398.

Volwerk, M., K.-H. Glassmeier, R. Nakamura, T. Takada, W. Baumjohann, B. Klecker, H. Rème, T. L. Zhang, E. Lucek, and C. M. Carr (2007), Flow burst-induced Kelvin–Helmholtz waves in the terrestrial magnetotail, *Geophys. Res. Lett.*, *34*, L10102, doi:10.1029/2007GL029459.

Voronkov, I., R. Rankin, V. T. Tikhonchuk, and J. C. Samson (1997), Nonlinear shear Alfvén resonances in a dipolar magnetic field, *J. Geophys. Res.*, *102*, 27,137–27,144, doi:10.1029/97JA02533.

Walker, A. D. M. (1987), Theory of magnetospheric standing hydromagnetic waves with large azimuthal wave number, I:

Coupled magnetosonic and Alfvén waves, *J. Geophys. Res.*, *92*, 10,039–10,045, doi:10.1029/JA092iA09p10039.

Walker, A. D. M. (2005), Excitation of field line resonances by sources outside the magnetosphere, *Ann. Geophys.*, *23*, 3375–3388, doi:10.5194/angeo-23-3375-2005.

Wright, A. N., and W. Allan (2008), Simulations of Alfvén waves in the geomagnetic tail and their auroral signatures, *J. Geophys. Res.*, *113*, A02206, doi:10.1029/2007JA012464.

Zelenyi, L. M., A. V. Artemyev, A. A. Petrukovich, R. Nakamura, H. V. Malova, and V. Y. Popov (2009), Low frequency eigenmodes of thin anisotropic current sheets and Cluster observations, *Ann. Geophys.*, *27*, 861–868, doi:10.5194/angeo-27-861-2009.

Zhang, T. L., W. Baumjohann, R. Nakamura, A. Balogh, and K.-H. Glassmeier (2002), A wavy twisted neutral sheet observed by CLUSTER, *Geophys. Res. Lett.*, *29*, 1899, doi:10.1029/2002GL015544.

Zhu, P., and J. Raeder (2014), Ballooning instability-induced plasmoid formation in near-Earth plasma sheet, *J. Geophys. Res.*, *119*, 131–141, doi:10.1002/2013JA019511.